Electronically stimulated desorption of neutral atoms from Ar films on Ru(001): Desorption mechanisms and energy-transfer processes derived from distributions of kinetic energy

E. Hudel, E. Steinacker, and P. Feulner
Fakultät für Physik E20, Technische Universität München, D-8046 Garching, Federal Republic of Germany
(Received 25 April 1991)

Desorption yields as well as kinetic-energy distributions of desorbing argon atoms were investigated for pure argon films of variable thickness (annealed and not annealed), and for Ar samples doped with N_2, O_2, and NO additives of (a) 1% and 5% concentration in the bulk, and (b) $\frac{1}{4}$ to $\frac{1}{2}$ monolayer on the surface. The preparation-dependent prevalence of different desorption processes is investigated. Bimodal energy distributions are obtained from clean, annealed samples which are drastically changed by dopants as well as lattice defects. From thick, annealed samples the yield ratio of fast to slow particles is found to be 1.6, which is much larger than reported for previous experiments. This indicates that perfect vacuum conditions are decisive for the study of such systems if mechanistic conclusions are to be drawn.

I. INTRODUCTION

For a large variety of solids electronic excitations caused by bombardment with photons, electrons, and fast light ions induce the desorption of particles. The elementary steps of these DIET (desorption induced by electronic transitions) reactions are (1) the primary electronic excitation, (2) the evolution of this electronic excitation including its modification by Auger processes, propagation through the solid, and localization, (3) the competition between the decay of the excitation and the acceleration of nuclei, and finally (4) secondary phenomena like sputtering of surrounding ground-state material by the fast particles originating from step (3). Films of rare gases on metallic substrates have been widely used as model systems for the investigation of DIET from weakly bound solids. Several theories have been developed for the description of the microscopic details of the DIET process for monolayers as well as for multilayers of rare gases on metals; these will be sketched in the following.

For *monolayers,* one established approach is the so-called Antoniewicz mechanism.[1] For physisorbed species, the basic steps are the primary ionization of an adparticle, its acceleration towards the surface, neutralization close to the surface, and desorption, if the sum of its potential and kinetic energies exceeds the binding energy in the ground state; this means that the lifetime of the ionic state has to exceed a critical value.[2,3] Different descriptions have been given of the real and imaginary parts of the potential for the ionic state which govern the movement to the surface, and the neutralization, respectively.[3] Another, purely quantal approach explains DIET from rare-gas monolayers on metals as due to the squeezing of the wave packet representing the adparticle by the electronically stimulated initiation of strong interactions with the surface;[4] here, the nuclear acceleration is a consequence of the uncertainty principle.[4] The experimental tests for all of these theories were comparisons of measured[5] and calculated[2–4] distributions of the kinetic energy $N(E_k)$ of the desorbing particles, as well as total desorption yields.

DIET from rare-gas *multilayers* or rare-gas solids (RGS's) was shown to be mainly caused by the excitation of excitons, their diffusion to, and their localization near the surface.[6,7] Experimentally, excitons can selectively be excited by photons.[8] For electronic stimulation with fast ions or electrons, ionization is the prevailing primary excitation. Excitons are then created in secondary steps via electron-hole recombination processes.[6] The desorption of particles is the consequence of the relaxation processes in the solid before, and after the decay of the localized electronic excitation. For atomic self-trapped excitons all nearest neighbors of the excited atom are symmetrically displaced.[8] For the light rare gases Ne and Ar, the interaction causing this displacement is repulsive.[7–9] If the exciton is localized at the surface, this electronically excited atom is instantaneously repelled into the vacuum by the forces resulting from its asymmetrical environment.[7,9] Electronically excited molecules (Ar_2^* excimers) whose electronically stimulated desorption has been detected in fluorescence experiments,[10,11] are also expected to be desorbed via this "cavity mechanism."[11] Calculations on this desorption mechanism for Ar atoms as well as excimers indicate that the kinetic energies of the desorbing particles are low.[12,13] While the predictions for this quantity vary considerably for different models of the interaction potentials between the excited atom and the lattice of the RGS, it is clear that the "center of gravity" is well below 100 meV for Ar* atoms.[12] For excimers, it is even lower[13] (according to a recent theoretical study, desorption of singlet state excimers via that mechanism can be expected from solid Kr as well, with extremely low kinetic energies[14]). The energy dissipated in the lattice during the expulsion of the particles is of the same order of magnitude as their kinetic energy, i.e., it is around the sublimation energy of solid Ar [78 meV (Ref.

15)]. Sputtering of ground-state material can be excluded, because this amount of energy is distributed to all nearest neighbors in nearly equal parts.[11–13] However, the calculations predict, for Ar* as well as for Ar_2^*, strong dependences of the kinetic energy E_k on the number of nearest neighbors, irrespective of the ansatz for the interaction potential.[12,13] E_k should decrease if the number of nearest neighbors is reduced, by, e.g., lattice imperfections.[12,13] Moreover, DIET of Ar_2^* species via the cavity mechanism from perfect crystals where the shell of nearest neighbors is complete has been predicted to be faster than the vibrational relaxation of the excimers by the emission of phonons, i.e., the excimers are desorbed vibrationally hot[13] (this vibrational excitation arises from the much smaller Ar—Ar bond length in the excimer than in the van der Waals crystal[6]). The subsequent dissociation by radiative deexcitation in the gas phase yields less fast fragments than for vibrationally cold excimers, where a total energy of about 1 eV is distributed to the two Ar atoms.[6,10] For imperfect samples the time of residence on the surface should be increased, and the kinetic energy of the fragments as well.[13]

A reaction sequence mainly causing DIET of ground-state atoms from RGS's has been labeled the molecular mechanism (Refs. 6 and 10, and references therein). Here, a molecular self-trapped exciton (i.e., a X_2^* molecule) is formed, and cooled to its vibrational ground state by phonon emission inside the lattice.[8] By its dissociative deexcitation, the excess energy of the order of 1 eV (Refs. 6 and 10) is distributed to the two atoms as described above. If its dissociative decay happens close to the surface, the collision cascade initiated by the two constituent atoms which each have about half an eV of kinetic energy can cause sputtering of surface atoms.[6,16–18] If one of the constituents of the molecular self-trapped exciton is an atom from the surface layer, it can desorb directly with its full kinetic energy.

Bimodel energy distributions have been observed experimentally for DIET from RGS's.[19–21] The high-energy maximum of them has been assigned to direct desorption, and the low-energy peak to erosion by collision cascades.[19–21] It has been shown that both the maximum energy release due to the radiative decay of the excimer, and the sputter yield depend on the crystallographic environment.[16–19] Lattice imperfections are therefore expected to influence $N(E_k)$ of particles desorbing via this mechanism as well.

Moreover, the branching into fast and slow particles reflects differences of the trapping rates for free excitons in the surface layer, and inside the bulk, respectively, because localization of the excitation with participation of atoms from the surface layer causes direct desorption.[8,10,19–22]

The dissociative neutralization of Ar_2^+ ionic dimers was suggested as a second decay channel delivering kinetic energy for desorption and sputtering.[6,10] However, from our experiments we estimate that the contribution of this reaction to the desorption of neutrals is small (see below). For the expulsion of minority species like fast electronically excited atoms[23] and excimers[10,24] which we do not consider in this study, it certainly is important.

Recording $N(E_k)$ of the outgoing particles obviously is a powerful method to investigate the microscopic details of the DIET process, and to verify different theoretical approaches, for monolayers as well as for multilayers of rare gases on metals. So far, only one experiment has been done for monolayers; its results are in good agreement with calculations.[3–5] For multilayers, data from three different experiments exist which show severe discrepancies concerning the height and the position of that maximum which is related to direct desorption, i.e., to the atoms from dissociating excimers.[19–21] Steinacker, Feulner, and Menzel reported for solid argon this peak to be of comparable area as that at low kinetic energy,[20] whereas O'Shaughnessy *et al.* obtained for it only a fraction of 12–14 % of the total desorption flux;[19] in the spectra of Pedrys *et al.*, such a maximum is completely missing.[21]

From photoelectron spectroscopy it is known that free excitons in rare-gas solids are preferentially trapped by the metal substrate and by impurities in the sample.[25] Therefore, one would expect that all desorption mechanisms involving the diffusion, the trapping, and the decay of excitons might strongly be affected by impurities, as well as—for thin layers—by the vicinity of the metallic substrate. Contaminants in the bulk or on the surface of the rare-gas films could be the cause for the discrepancies quoted above. An indication for such a reason are the different vacuum conditions of the previous experiments. The data from Ref. 20 were recorded at a base pressure of less than 1×10^{-11} mbar, those of Refs. 19 and 21 under less perfect UHV conditions ($p<1\times10^{-9}$ mbar). However, at 1×10^{-9} mbar approximately 2% of a monolayer are adsorbed from the residual gas within only one minute.

To investigate the influence of such kinds of "imperfections" of the RGS's on $N(E_k)$ of the particles desorbed by electron impact was the goal of this study. To separate effects of different origins, the influences on $N(E_k)$ of (a) dopants in the bulk (O_2,N_2,NO), (b) surface layers of molecules (O_2,N_2,NO), (c) lattice imperfections due to insufficient annealing of the films after dosing at low temperature, and (d) of the vicinity of the metal substrate were separately monitored.

II. EXPERIMENT

The $N(E_k)$ data were acquired in a UHV chamber equipped with a combination of a liquid-nitrogen-trapped diffusion pump, an ion pump, and a titanium sublimation pump. During the measurements, the pressure was always below 10^{-11} mbar. Auxiliary measurements on the segregation behavior of dopants in the RGS's were performed with synchrotron light at the SX-700-I beam line at BESSY, Berlin (see Sec. III C) in a second chamber. The vacuum conditions as well as the sample preparation techniques utilized in both experiments (see below) were identical.

$N(E_k)$ data of the desorbing particles were recorded by a time-of-flight (TOF) apparatus which partly has been described in Refs. 5 and 20. Its essential components, see Fig. 1, are (a) a drift tube with three skimmer apertures,

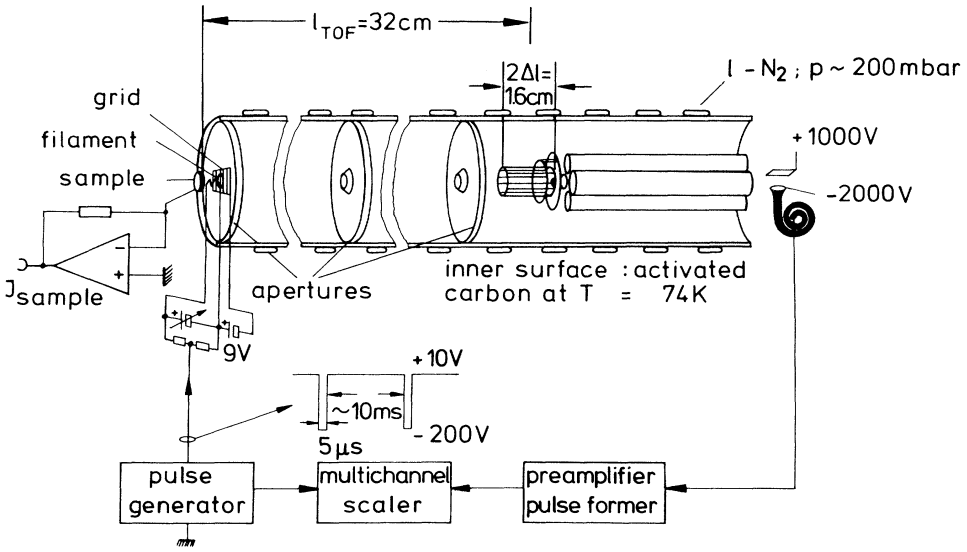

FIG. 1. Time-of-flight apparatus. See text for details.

internally covered with activated carbon—after cooling to 74 K the Ar partial pressure in this tube was below 10^{-13} mbar; (b) a thoriated tungsten filament serving as electron emitter in front of the entrance skimmer of this tube; (c) a quadrupole mass spectrometer (QMS) equipped with an electron impact ionizer of high yield mounted inside the tube behind the last skimmer. To record spectra, the sample was positioned in front of this assembly and irradiated with electron pulses by biasing the filament negatively for 5 μs; the electron energy was always 200 eV. The length of the flight path between the sample and the ionizer was 32±0.8 cm; its scatter, which is the limiting factor of the energy resolution of this setup, is due to the axial extension of the active volume of the ion source, see Fig. 1. The pulses from the channeltron of the QMS were accumulated with a multichannel scaler (MCS) with 512 channels [in Refs. 5 and 20, a MCS with only 256 channels was used; the energy resolution and the accuracy of the calibration particularly for the high-energy tail of $N(E_k)$ obtained here are better than in Ref. 20, see below]. Its dwell time was set equal to the length of the electron pulses. The raw data were corrected for the transit time of the ions through the QMS, and for the background due to the residual gas pressure inside the TOF tube. This constant background level was derived from the time-independent part of the QMS signal between the electron pulse and the leading edge of the $N(t)$ trace, and it was in perfect agreement with the signal for very long flight times, i.e., after the trailing edge of $N(t)$, see Fig. 2(a) (we emphasize that because of the good pumping speed of our TOF tube it was *not* necessary to subtract any time-dependent background as described in Ref. 19; the determination of the correct curvature of such a time-dependent background is difficult and artifacts can easily be created). To keep the background pressure low even for excessive gas load, after the dosing of about 300 layers (see below) the TOF tube was rapidly heated to 130 K, and subsequently cooled to its base temperature. Such cycling perfectly regenerated its pumping properties.

The TOF data were then converted to $N(E_k)$ spectra as described in Refs. 5 and 20 [see Fig. 2(b); after applying a Fourier smooth, traces as shown in Fig. 2(c) were obtained]. The correct performance of all computer routines used for the processing of the data was checked

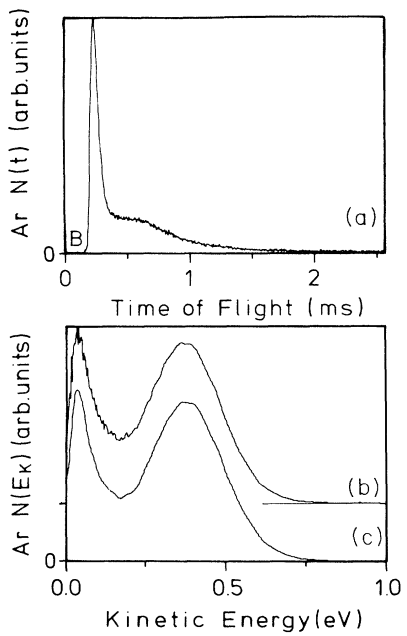

FIG. 2. (a) A typical $N(t)$ spectrum obtained from a 250-ML thick Ar film. The background was obtained from the range labeled B (see text). (b) $N(E_k)$ trace obtained from the data shown in (a). (c) The spectrum shown in (b) after the application of a Fourier smooth.

with synthetic spectra. The electronic excitation rates were always low enough to exclude thermal effects, or interactions of the desorbing particles in the gas phase (adiabatic expansion). Due to the geometry of the setup, only particles desorbing within a cone of ± 0.4 degrees around the detector axis were collected.

To obtain uniform distributions, all samples were prepared by dosing gases through a microchannelplate doser onto the ruthenium (001) substrate cooled to 10 K by a liquid-helium cryostat. Pure Ar samples, as well as alloys of argon and molecules, were dosed from either pure Ar or gas mixtures kept at constant partial pressure ratios in the inlet system. This was operated under constant flow conditions for optimum purity of the dosing gases (the nominal purities were 98% for NO, and 99.98% for all the other gases). The temperature of the samples was variable between 10 and 1600 K. Constant temperatures (± 0.05 K) as well as constant ramp rates from 0.1 to 20 K/s could be maintained by an electronic controller.[15] The substrate was cleaned by heating in oxygen and sputtering with argon. Its cleanliness and crystallographic perfection were checked with low-energy electron diffraction (LEED), Auger electron spectroscopy (AES), and temperature-programmed desorption (TPD) of Xe [for this adsorbate a maximum is visible in TPD which is correlated to an incommensurate-commensurate phase transition; it is strongly suppressed by impurity concentrations of less than 1% (Ref. 15)].

The calibration of the thickness of the samples was derived from TPD spectra; the film thickness Θ is given in multiples of the amount of particles which are adsorbed on the substrate in the first layer [=1 monolayer (ML)]. Pure monolayers were prepared by dosing 10% in excess, and heating to the minimum in TPD between monolayer and multilayer desorption.[15]

III. RESULTS

A. Dependence of $N(E_k)$ and the desorption yield on the thickness of the films

In our first experiment we prepared pure argon samples with thicknesses from 1 ML (preparation as described above) up to 250 ML. After dosing, the films were annealed by ramping the temperature up to 20 K with 0.5 K/s. From these samples we measured $N(E_k)$ of the argon atoms desorbed by excitation with electrons of 200 eV. The results are shown in Fig. 3. The shape of $N(E_k)$ as well as the desorption yield depend on the thickness of the films. For less than 7 ML, the distributions exhibit only one maximum. This maximum lies at 55 meV for the monolayer, and shifts to lower kinetic energies with increasing Θ; simultaneously, the desorption yield is decreased (see below). For 5 ML, the most probable kinetic energy $\hat{E}_k$ of the desorbing particles is 43 meV. Starting at 7 ML, a second maximum grows in at 385 ± 5 meV, which is strongly enhanced with increasing film thickness, while its energetic position is unchanged. For convenience, we will refer to these maxima at ≈ 40 and 385 meV as L (for low energy), and H (for high energy) peaks, respectively. In our experiments, saturation

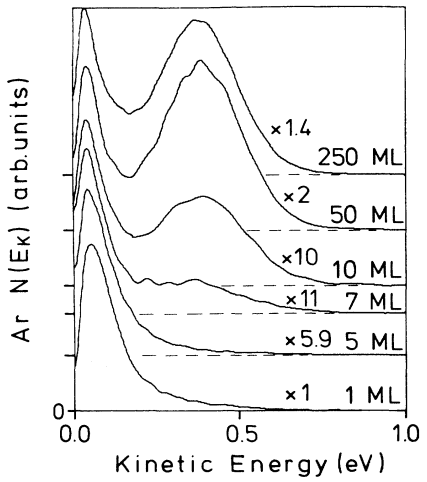

FIG. 3. Energy distributions of Ar atoms desorbed from Ar films of various thicknesses. The films were annealed at 20 K (see text). The heights of the L maxima are normalized to that obtained for the monolayer; the scaling factors are given in the figure.

was obtained at approximately 250 ML. At that coverage, the L peak was at 40 meV.

To evaluate the individual areas of these two maxima, a line proportional to $\exp(-E_k/\varepsilon)$ was fitted to the trailing edge of the L peak, see Fig. 4. For each Θ, the parameter ε was chosen for minimum deviation. We emphasize that such an exponential decrease is not the functional dependence on energy expected from the classical collision cascade model. From this one would expect a Thompson distribution with an asymptotic behavior like E_k^{-2};[6,26] such a function exhibited much larger deviations from the experimental curves than that from Fig. 4. This could be an indication that the L maximum originates partly from other processes than sputtering by fast particles. Also, results of microscopic calculations indicated that particles indirectly desorbed via the molecular process should possess a steeper decrease of $N(E_k)$ for high

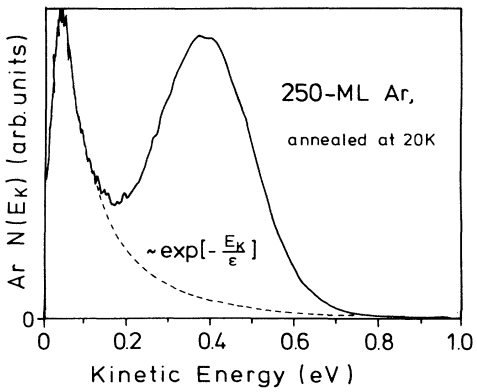

FIG. 4. Deconvolution of the L and H peaks was obtained by fitting the trailing edge of the L peak with an exponential decay function (dotted line; see text).

kinetic energies than predicted by the Thompson formula.[16] The parts of $N(E_k)$ above and below this fitted line, respectively, were then taken as the contributions of the two maxima. The results are shown in Fig. 5.

The desorption yield is high for monolayers. In Ref. 5, an average escape probability P (Ref. 27) of 64% had been derived for electrons of 200 eV, i.e., the branching of a primary ionization event into desorption was 0.64. This value was corroborated here by homogeneously irradiating saturated Ar monolayers whose atom density is known[15] with electrons of 200 eV, and measuring the coverage by TPD before and after the bombardment. Using the ionization cross sections for Ar from Ref. 28, a P of 60% was derived in very good agreement with the findings of Ref. 5. We therefore take the DIET yield from the monolayer as a standard and refer to it by setting it to unity in the following figures. For films that are 5 ML thick, the desorption yield is reduced to a value of about 0.12 times the yield for one monolayer. The yield passes through a minimum between 5 and 7 ML, and rises again if Θ is increased beyond 7 ML. Additional dosing then enhances both maxima. For 250 ML, the total desorption yield is larger than that for the monolayer by a factor of 1.8, and the ratio of the L and H areas is 1:1.6 (for the derivation of these ratios, we assume equal angular distributions for all of these contributions; the validity of this assumption is discussed in Sec. IV A).

B. Influence of annealing

In Fig. 6, $N(E_k)$ spectra obtained from samples of 50 and 250 ML dosed at 10 K, and from samples annealed after dosing as described above, are compared. For both coverages, the overall desorption yield is larger for those samples which were annealed after dosing. For the films which had not been annealed, the L maximum was found to be shifted to lower kinetic energy by ≈ 10 meV. The branching into fast and slow particles is also affected. Compared with the annealed films, the L peak is less strongly depleted than the H maximum at 385 meV, see Fig. 6. Coverage-dependent yield measurements exhibited a delayed decrease of the desorption yield between 1 and 7 ML for these films, compared to those which had been annealed at 20 K. At 5 ML, annealing was found to *decrease* the desorption yield by a factor of 2.7, and to shift the peak energy from 48 to 43 meV.

C. Influence of N_2, O_2, and NO impurities, (a) doped into the bulk, and (b) adsorbed on the surface, on $N(E_k)$, and on the desorption yield obtained from Ar films

To investigate the influence of impurities on DIET from Ar films, two different types of samples were prepared and studied. Version (a) was alloys of Ar and the diatomic molecules N_2, O_2, and NO. These films were prepared by dosing mixtures of Ar and the respective dopant simultaneously onto the sample through the microchannelplate doser. Samples with dopant concentrations of 1% and 5% were used for the $N(E_k)$ experiments. The temperature of the substrate during the exposure was 10 K. Version (b) was pure, not annealed Ar films which had been covered with surface layers of the doping gas. These surface layers were prepared by dosing an amount of the second constituent onto the Ar film such that coverages in the range of 0.25–0.5 ML were obtained.

The type (a) samples were checked with angular-resolved electron spectroscopy for segregation of the dopants in the surface region. For nominal bulk concentrations of 1%, Auger spectra for normal and grazing exit angles were recorded. To obtain maximum sensitivity, the photon energies were set to the π resonances of

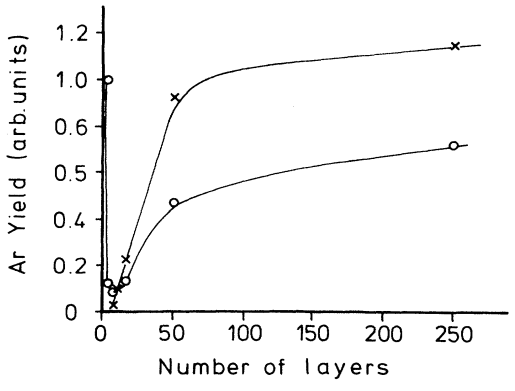

FIG. 5. Relative contributions of (×) fast (H maximum), and (○) slow particles (L maximum) to the desorption yield for annealed Ar films of various coverages (the lines are only intended to guide the eye and do not represent a functional dependence).

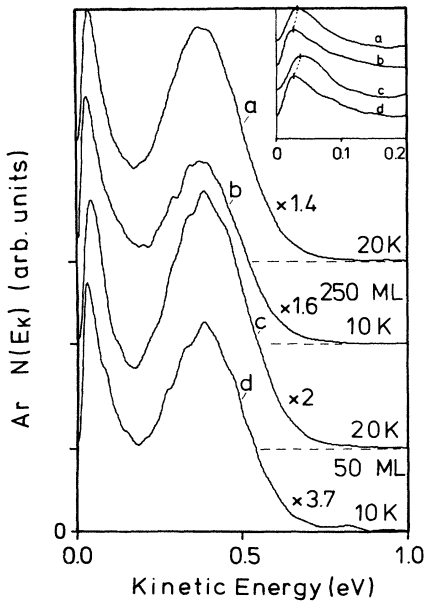

FIG. 6. Comparison of Ar $N(E_k)$ curves obtained from Ar films annealed at 20 K, and films dosed at 10 K. The inset shows the range from 0 to 0.2 eV kinetic energy on an expanded energy scale.

the respective molecules. For nominal bulk concentrations of 50% [which were not used for our $N(E_k)$ investigations reported here], angular-resolved ultraviolet photoelectron spectroscopy (UPS) spectra were taken. Here, a photon energy of 150 eV was selected to minimize the mean free path of the photoelectrons and to optimize the surface sensitivity. For samples with [Ar]:[X]=1:1, depleted concentrations of the dopants on the surface were observed for all of the three molecular gases. Whereas for the bulk samples density fractions close to the nominal concentration of 50% were found (with absolute photoionization cross sections taken from Ref. 29, and the elastic mean free paths for the electrons estimated from total ionization cross sections for electron impact from Ref. 28), the surface concentration was found to be only 40% for nitrogen, 25% for oxygen, and 22% for nitric oxide. In the case of [Ar]:[X]=99:1, however, the fractions of host and dopants were observed to be identical for the bulk and for the surface. We assume that these results hold also for the films with fractions [Ar]:[X]=95:5.

The $N(E_k)$ traces obtained for Ar atoms from such 50-ML-thick alloyed and surface-covered samples are shown in Figs. 7–9. For comparison, $N(E_k)$ for Ar obtained from a pure Ar film of 50 ML dosed at 10 K is shown at the top in each figure.

It is obvious that for the doped films the H peak is always smaller than the L peak; for 1% as well as 5% O_2 in the bulk, or 0.25–0.5 ML of this gas dosed onto the surface, it is completely suppressed (Fig. 7). For bulk mix-

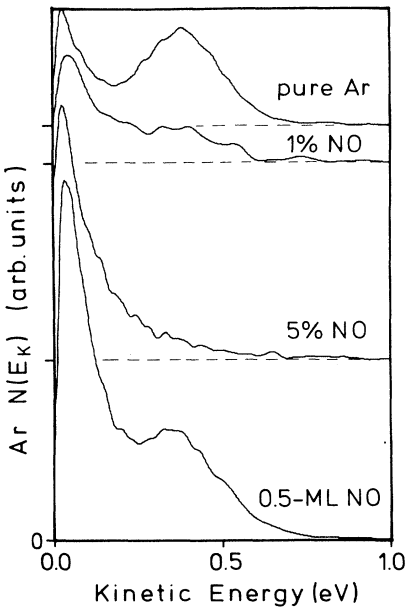

FIG. 8. Ar energy distributions from Ar samples (50 ML) doped with 1% and 5%, respectively, of NO in the bulk, and from films of pure Ar covered with 0.5 ML of NO on the surface. For comparison, a $N(E_k)$ trace obtained from a clean Ar sample dosed at 10 K is shown at the top.

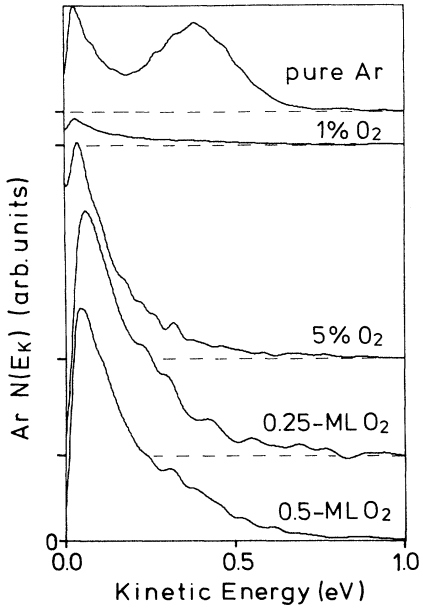

FIG. 7. Ar energy distributions from Ar samples (50 ML) doped with 1% and 5%, respectively, of molecular oxygen in the bulk, and from films of pure Ar covered with 0.25 as well as 0.5 ML of oxygen on the surface. For comparison, a $N(E_k)$ trace obtained from a clean Ar sample dosed at 10 K is shown at the top.

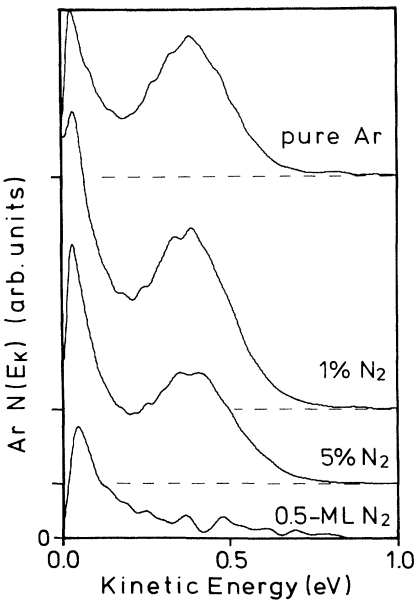

FIG. 9. Ar energy distributions from Ar samples (50 ML) doped with 1% and 5%, respectively, of molecular nitrogen in the bulk, and from films of pure Ar covered with 0.5 ML of nitrogen on the surface. For comparison, a $N(E_k)$ trace obtained from a clean Ar sample dosed at 10 K is shown at the top.

tures with 1% of NO, a rest of the H peak is still visible, see Fig. 8. If the NO concentration is raised to 5%, it vanishes; but it is clearly discernible for 0.5 ML of NO on the surface, though at slightly lower $E_k = 355$ meV. Surprisingly, 1% of N_2 *increases* the H peak beyond the height obtained for pure, not annealed Ar samples (see Fig. 9; the increase of L, however, is still larger). 5% of N_2 in the bulk deplete the H maximum, and 0.5 ML on the surface suppress it.

The areas under the traces in Figs. 7–9 indicate that the total Ar desorption yields are strongly affected by dopants as well. With the exceptions of 1% of O_2 in the bulk, and 0.5 ML of N_2 on the surface (see Figs. 7 and 9), the DIET yields are higher for these alloyed or covered samples than for the pure Ar films. Because of the depleted H intensity, this means that the L maximum is increased in most of these cases. Coverage-dependent yield measurements, which have been performed for samples with 5% of O_2 in the bulk, exhibited leveling off of the desorption rate at about 7 ML only, i.e, saturation occurs for much thinner films than for pure Ar samples, which indicates that for these alloys the diffusion of the primary excitation is suppressed.

During the electron bombardment of the samples with bulk dopants we noticed changes of the shapes of $N(E_k)$, see Fig. 10. Extended irradiation caused spectra which were similar to those obtained from pure, not annealed Ar films, see Fig. 10. Particularly the H peak reappeared, though its fraction even for very high electron doses was always below that from samples of pure Ar. The electron doses which were necessary to partly cancel the influence of molecular dopants were larger for O_2 than for N_2, see Fig. 10.

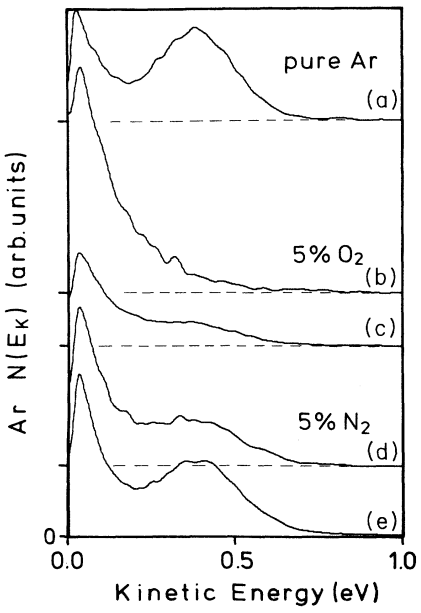

FIG. 10. Influence of extended irradiation of alloyed Ar/O_2, N_2 samples with electrons; exposures q: (b), (d) $q < 20$ μAs, (c) $q = 635$ μAs, (e) $q = 105$ μAs. (a) For comparison, a $N(E_k)$ spectrum obtained from a clean Ar sample dosed at 10 K is shown.

We mention that small amounts of neutral Ar dimers were detectable for the clean as well as for the alloyed samples (for films of pure Ar, the Ar_2 signal was lower than the Ar signal by a factor of 1.8×10^{-3}). The $N(E_k)$ traces from these were centered at about 30 meV for the alloys; for samples of pure Ar, $\hat{E}_k$ was slightly lower. The width was around 50 meV. Admixtures of 5% of NO and O_2 increased the dimer signal by a factor of 3; 5% of N_2 had no influence on the desorption yield.

IV. INTERPRETATION AND DISCUSSION

A. Films of pure argon

The observed variations of $N(E_k)$, as well as of the total desorption yield with film thickness, can be interpreted in terms of the mechanism presented in the Introduction. $N(E_k)$ and yield data for monolayers have been discussed previously.[2–5] In particular, the desorption yield data obtained here corroborate those of Ref. 5. The $N(E_k)$ trace is similar too, but the maximum is shifted to lower E_k by 5 meV, and the contribution of the trailing edge is slightly smaller than in Ref. 5; at $E_k = 0.2$ eV, the relative desorption yield obtained here is only 81% of that in Ref. 5. The origin of these discrepancies is not completely clear to us. Similar deviations for the multilayer data (see below) indicate that due to the better energy resolution obtained here the energy scale given in Refs. 5 and 20 has to be corrected; the E_k values given there probably are too high by about 10%. We emphasize that the critical quantity of our experimental setup, i.e., the length of the TOF tube, was determined very carefully in the present study.

Both DIET mechanisms suggested for monolayer systems, the Antoniewicz process[2,3] as well as the quantal approach,[4] require the vicinity of the metal surface. One could imagine that even for thin multilayer systems fast particles originating from monolayer processes in the first layer on the metal might erode overlayers by sputtering. Considering the monolayer $N(E_k)$ spectra, and the sputter yield versus excitation depth results given in Fig. 1 of Ref. 16 (the results of Ref. 17 are comparable, the yields being lower by about 30%), we estimate that such contributions will be important only for films of less than 5 ML. The dip of the DIET yield versus film thickness for samples of 5–7 ML, see Fig. 5, most probably is due to this decrease of the contribution from the monolayer mechanisms, and to a delayed onset of the multilayer processes which all involve the evolution of excitonic excitations (see above). The larger electron stimulated desorption (ESD) signal at 5 ML from the films which have *not been annealed* probably stems from dilute areas of the Ar film where the contributions of the monolayer mechanisms via collision cascades is still strong, i.e., it is a consequence of the inhomogeneous thickness of such samples. We emphasize that even for the annealed samples the minimum of the L maximum is obtained beyond $\Theta = 5$ ML. This indicates contributions of DIET processes originating at the metal-RGS interface for this coverage range as well. Because sputtering by particles stemming from the first layer on the metal can be excluded (see above), we tentatively explain these by an An-

toniewicz sequence involving ions created in the second or third layer above the metal interface which still feel strong attraction by their image force.

For a better understanding of the contributions of the exciton-based mechanisms to the ESD signal for films of various thicknesses we briefly summarize the time scales which are important for their dynamics. The primarily created free excitons in solid Ar have a mean lifetime of about 10^{-12} s until they self-trap.[8] An atomic self-trapped exciton on the surface can immediately [i.e., in about 10^{-11} s (Ref. 12)] lead to desorption via the cavity mechanism,[7,12,13] while desorption via the molecular process requires complete vibrational relaxation of the involved molecular self-trapped exciton for maximum kinetic energy of the fragments.[6,10,19–22] In Ar, this vibrational relaxation takes about 0.5×10^{-9} s.[30] For dipole-allowed transitions, the lifetime of the electronic excitation until its radiative decay is also of the order of nanoseconds.[11] However, photoelectron studies have shown that all these excitations can be quenched by the substrate, as well as by impurities, via long-range Förster-Dexter energy transfer processes.[25,31,32] The related relaxation time for the first layer on the metal (where deexcitation by charge-transfer reactions adds to the Förster-Dexter energy transfer[33]) is about 10^{-14} s;[33] for excitations more remote from the metal interface, it decreases like d^{-3}, with d the spacing between the surface of the substrate and the excited particle.[33,34] This was confirmed by photoemission measurements of Ophir *et al.* where the dependence of the photoemission yield from RGS's on metals for excitation of excitons could be explained in terms of exciton diffusion, and energy transfer to the substrate by the mechanisms quoted above.[25] This means that for thin layers the *fast* cavity process is less strongly quenched by energy transfer to the metal than the *slow* molecular mechanism. This is corroborated by PSD (photon stimulated desorption) data which for thin films show the prevalence of surface excitons for DIET, which mainly cause desorption via the cavity mechanism.[35] We therefore conclude that the $N(E_k)$ trace for annealed films of 5 ML, as well as the L section of the trace for 7 ML (see Fig. 3), represent mainly the kinetic-energy distribution due to DIET via the cavity process with some contributions from reactions of the Antoniewicz type. The most probable energy, $\hat{E}_k=43$ meV, is well within the energy range obtained by the model calculations in Ref. 12. We emphasize that particularly the L part of the 7-ML curve in Fig. 3 is indicative of the curvature of the interaction potential between the excited atom and the lattice of the RGS, because contributions from sputtering by fast particles originating either from ion-metal interaction, or decaying excimers (the H peak is still small, see below), should be negligible.

The H peak in $N(E_k)$ at 385 meV which grows in if Θ exceeds 7 ML has been assigned previously to direct desorption via the molecular mechanism from decaying excimers.[19,20] For clean, well-annealed samples of more than 50 layers it contributes about 62% to the total desorption yield. Our results in Sec. III C show convincingly that the previously mentioned discrepancies concerning its area are certainly due to surface or bulk contaminations stemming from insufficient vacuum conditions. The peak energy is constant at 385 meV, irrespective of the density of crystallographic defects, see Sec. III B, and of the presence of dopants which deplete it (except for the energy shift caused by NO which will be discussed below in Sec. IV B). However, if dissociation of Ar_2^* molecules in the gas phase which are desorbed via the cavity process would make an important contribution to this maximum, the most probable energy should strongly depend on the preparation of the sample. The reason is that the time of residence of the excimers on the surface, which governs via the degree of their vibrational relaxation the maximum kinetic energy of the fragments created in their radiative decays, strongly depends on surface imperfections.[13] From these findings we conclude that the H peak stems from vibrationally relaxed excimers which decay on the surface of the RGS, i.e., it is due to the direct desorption channel of the molecular mechanism. Its sensitivity to (a) the vicinity of the metal, and (b) impurities can be easily understood by the long lifetime of the excitation which is necessary for the vibrational relaxation. In Ref. 10, fluorescence light of the M band at 9.7 eV which is indicative of radiative deexcitation of vibrationally cold Ar_2^* molecules[8] was seen only for $\Theta>60$ ML. This is not in direct contradiction to our results, because deexcitation by radiation is not a prerequisite for the molecular process. If such an excimer which is already cooled to its ground state by phonon emission (a reaction which is faster than the radiative decay, see above) dissociates by energy transfer to the metal via the Förster-Dexter process, identical $N(E_k)$ spectra as for the radiative decay will be obtained, but no 9.7-eV fluorescence light will be observed.

The H peak is found here at lower kinetic energy than in Refs. 19 and 20. The difference between our present result and that given in Ref. 20 is of the same magnitude as the deviations obtained for the monolayer (see above); it is explainable by an incorrect calibration of the energy scale in Ref. 20. In Ref. 19, the high-energy peak was found at 460 meV for excitation with electrons, and at 540 meV for stimulation with He^+. We have no explanation for this discrepancy. We emphasize that our result (385 meV) would fit the theoretical energy distribution obtained from molecular dynamics calculations in Ref. 19 better than the experimental data given there.

The increase of the L maximum in $N(E_k)$ which parallels that of the H peak must be due to indirect desorption via sputtering by the fragments of dimers dissociating underneath the surface.[6,10,16–18] Comparing its areas for 5 ML, where the cavity process dominates,[13] and 250 ML, we conclude that the L peak for the latter coverage is governed by collision cascade processes. In Ref. 16, the sputter yield as a function of the decay depth of the dimer has been calculated (see Fig. 5 in Ref. 16). Assuming that for thick layers sputtering is the only contribution to the L maximum, we estimate from the L:H ratio of 1:1.6 that the probability for molecular trapping of excitons in annealed samples is enhanced on the surface by a factor of ≈7 compared to the bulk, i.e., the surface is an effective exciton trap (if we include the contribution of

the cavity mechanism to the L maximum, which, by definition, means trapping of excitons in the first layer, this number would be even increased). In Ref. 22, an enhancement of the trapping rate in the surface layer by a factor of 4.7 was derived from the surface desorption yield (our H maximum) obtained in Ref. 19, and electronic transport properties. This number seems to be not significant because the data in Ref. 19 most probably are influenced by impurities (see above). In the presence of molecular overlayers localization of the electronic excitation would enhance the L and not the H peak (see Figs. 7–9, and below), i.e., we expect the total desorption yield given in Ref. 19 to be increased, the contribution of the H maximum however to be decreased by contaminants. This is corroborated by the finding that application of our evaluation procedure sketched above, which is based on the ratio of both maxima and the sputtering properties alone, to the Ar data of Ref. 19, gives a surface enhancement for the trapping of only ≈ 2.

All the previous publications on DIET via the molecular process also discuss the possibility of both direct desorption and collision cascade mediated erosion by the decay of ionic dimers (Ref. 10, and references therein). The amount of kinetic energy, which is liberated by curve crossing from the bonding part of the Ar_2^+ to the antibonding branch of the Ar_2^* potential, which causes dissociation into Ar* and Ar of the dimer, should be similar to that obtained for the decay of Ar_2^*, though not identical.[10] The constancy of the energetic position of the H maximum irrespective of the preparation and the film thickness in our opinion rules out such a decay channel. We mention that efforts to detect Ar_2^+ in the RGS by photon spectroscopy failed.[36] We think that the reason for this is that the charge in the solid is not localized on a dimer, but on a trimer, or even on larger entities. This is supported by calculations for ionic clusters, which favor the trimer, and for larger clusters even the Ar_4^+ as cluster kernels.[37] Because of the larger Ar—Ar bond lengths and the smaller binding energy per atom of these polyatomic ionimers,[38] the energy liberated at the decay is reduced compared to Ar_2^+, and is distributed among more atoms. We therefore conclude that such processes could contribute only to the L, but not to the H maximum.

From samples not annealed after dosing, $\hat{E}_k$ for the L contribution is decreased, see Sec. III B. In the collision-cascade model the position of the sputter maximum of the energy distribution is proportional to the binding energy of the atom on the sample surface.[16–18,26] In the case of defects the binding energy is smaller than for a perfect sample. This means that the sputter peak should be shifted to higher energies by annealing. However, this enhancement of $\hat{E}_k$ can also be understood by the increase of the kinetic energy of the atoms desorbed via the cavity mechanism. The computer simulations of Ref. 12 showed that the kinetic energies of the desorbing atoms are lower for incomplete shells of nearest neighbors. This means that annealing again should shift $\hat{E}_k$ of the L peak to higher energy. For layers of medium thickness, both effects might contribute to the observed differences in energy. For thick layers with saturated desorption yield, the first mechanism is expected to dominate as discussed above. The generally reduced desorption yield observed for samples not annealed after dosing must be due to the reduced diffusion length of the excitons. A not annealed sample has more defects than an annealed one and so the mean free path for excitations is shorter. Therefore the probability for an exciton to reach the surface and be trapped there decreases, and its decay cannot contribute to DIET.

The saturation behavior of the desorption yield with increasing Θ which is a consequence of the spatial exciton density due to diffusion is similar to that observed in Ref. 10. The total desorption yield derived by comparison of the $N(E_k)$ from monolayers and multilayers is surprisingly low compared to studies where fast light ions were used for the electronic excitation.[10] With gas phase data for the ionization cross section[28] we obtain 0.25 desorbing Ar atoms per incident electron. This is much less than obtained with excitation by light ions or fast electrons.[10,19,22] This finding would be understandable if the angular distributions would be very different for monolayers and multilayers, i.e., if DIET would be peaked in forward direction from monolayers and isotropic from multilayers. However, for the particles which are indirectly desorbed via the molecular mechanism calculations of Garrison and Johnson[16] predict angular distributions which are only 30° wide [full width at half maximum (FWHM)]. In our experiment we could change the exit angle only by ±5°. This did not change the L:H ratio, whereas the depletion of the signal when recording off the surface normal was compatible with the widths given above. The angular distribution of DIET from Ar monolayers has not been measured. Data from physisorbed N_2O where the mechanism of stimulated desorption should be similar, and where a FWHM of 66° was found,[2,39] indicate that the angular distribution for the monolayer should be broader than that for the multilayer. We therefore believe that the value given for the desorption yield above is not too small. The fact that it is so much lower than those for penetrating particles must be explainable by diffusive draining of excitons from the surface part of the film, where they are created, to its interior and finally to the substrate. We recall that the primary electrons of 200 eV lose their energy completely within a layer of about 40 Å on top of the RGS because of their large ionization cross sections.[28] No efforts were made to calculate their resulting spatial density distribution (for excitation with electrons of higher energy, such a study for Ar is reported in Ref. 40).

B. Alloys, and surface-covered Ar samples

As already pointed out, the discrepancies concerning the shapes of previously obtained $N(E_k)$ data can be explained by impurities, the dramatic influence of which on $N(E_k)$ was shown in Sec. III C. Though varying for different species, they all tend to deplete the H to L ratio, i.e., the branching into direct desorption from dissociating excimers. Even the total absence of the H maximum as obtained in Ref. 21 can be caused by surface layers of much less than 1 ML. We emphasize that even extended

bombardment of alloys with electrons does not restore the high-energy peak completely. This indicates that the atomic dopants which probably are formed from the primarily incorporated molecules also modify the dynamics of the microscopic details of the DIET reaction (see also below). Such influences have previously been observed in measurements of the luminescence and the total desorption yield.[10] Beyond the conclusion that best vacuum conditions are required for the investigation of such samples, we want to understand the mechanisms of these modifications of $N(E_k)$ by dopants, at least qualitatively.

Obviously there is a transfer of the electronic excitation from the argon to the additives like in thin samples from the Ar to the substrate. This transfer probably proceeds via the Förster-Dexter mechanism.[10,25,31,32] The better the excitation energies of the interacting partners coincide, and the closer the particles are, the more effective is this mechanism; for partners of distance R, the transition probability is proportional to R^{-6}.[31,32] This means that the transition probability strongly increases with the concentration of the dopants. Two energy regimes are important for our considerations of the processes in solid Ar: (a) the range from 12.1 to 14.2 eV for the deexcitation of free excitons in the bulk, which govern the transport of electronic excitation to and from the surface, and (b) the range from 9.7 to 12.1 eV for vibrationally relaxed and relaxing excimers in the surface, which contribute by their decay to the H peak. The time scales which are important here have been mentioned in Sec. IV A.

Other possible processes than electronic deexcitation via long-range dipole processes with the additives are charge-transfer reactions,[33] and the formation of transient molecules from excitonically excited hosts and adjacent dopants. Such reactions have been observed in near-edge x-ray-absorption fine-structure measurements of the Ar $2p_{3/2}^{-1}4s^{+1}$ excitation from Ar/O_2 (Ref. 41) and Ar/NO mixtures (this work). The resonance was then observed to be broadened and shifted in energy.[41] This was explained by charge-transfer reactions from argon to the neighboring molecules during the excitation step,[41] leading to the formation of $(O_2Ar)^*$ and $(NOAr)^*$ intermediates. Such results were not obtained for alloys of Ar and N_2. We assume that similar processes can proceed for valence excitations as well, because the energetic positions of the Ar $4s$ final state are nearly identical.[8,41] The auxiliary UPS measurements described in Sec. III C showed that the $1\pi_g$ level of O_2 as well as the 2π of NO can be ionized by an Ar ($n=1$) exciton; for the ionization of the NO 2π even the energy of a vibrationally cold Ar_2^* suffices. However, ionization of a N_2 molecule by deexcitation of an Ar($n=1$) exciton is impossible (see also Ref. 10); but the available energy is sufficient for neutral electronic excitations which will be discussed in the following.

For these excitations, we consider the energy range between 12.1 and 14.2 eV first. It is particularly important for N_2, because NO and O_2 will be preferentially ionized. For gas-phase N_2, many dipole allowed, nondissociative transitions from the ground state $X\,^1\Sigma_g^+$ to excited states with $^1\Sigma_u^+$ and $^1\Pi_u$ symmetry lie in this region.[42] For energies below 12 eV there is only one transition for N_2: $a\,^1\Pi_g \leftarrow X\,^1\Sigma_g^+$ at 8.5 eV. It is dipole forbidden ($g \leftarrow g$). For O_2 there is one dipole-allowed transition in this energy range ($B\,^3\Sigma_u^- \leftarrow X\,^3\Sigma_g^-$) which leads to dissociation.

With this information we can try to interpret the observed results. Obviously two different processes are important. The first is the transition of the excitation energy from the argon to the additive in the bulk of the RGS; it causes shortening of the mean free path of mobile excitations, and reduction of the number of excitations which are available for DIET near the surface. This concept has been derived before by Reimann, Brown, and Johnson from erosion yields obtained from Ar films containing small amounts of oxygen.[10] The second process concerns the enhancement of the localization probability for the excitons in the surface layer and the modification of the processes which supply the kinetic energy for the desorption of particles. Localized Ar_2^* excimers, e.g., can be deexcited before they are vibrationally relaxed, and the H maximum can be suppressed. In addition, fast fragments of dissociating molecules or excited complexes of molecules and rare-gas atoms could contribute especially to the sputtering channel. In the following we assume that for samples with 1% of additives influences on the transport, and for samples partially covered with molecules trapping and desorption phenomena are preferentially important. Samples doped with 5% should show a combination of both.

1% of O_2 or NO lead to a reduction of the desorption yield, although surface layers of both gases enhance the yield (the results for oxygen are in good agreement with those from Ref. 10). This means that oxygen and nitric oxide reduce the mean free path of excitations in the bulk, probably via their ionization by the free excitons and, possibly, the formation of transient ionic clusters. On the other hand, 1% of nitrogen in the bulk *enhances* the yield although from N_2 *covered* samples it is considerably *depleted*, indicating that no additional process which could contribute to the transfer from electronic to kinetic energy is introduced by this dopant. Obviously, ionization of the additives is much more important than neutral, nondissociative excitations as in the case of N_2. The reason for the enhancement of the DIET yield by 1% N_2 is not clear. Since the Ar signal is nearly as large as from annealed pure argon samples we tentatively explain this phenomenon by deactivation of lattice defects by N_2 molecules; this implies that the trapping probability of an exciton at a lattice defect is larger than at a N_2 molecule. The conspicuous reduction of the yield by 5% N_2 (and the fast increase during electron bombardment) possibly is due to N_2-N_2 neighbors. The localization probability at these van der Waals dimers could be larger than at single molecules in the argon matrix. They would preferentially trap the excitons, and be dissociated and made ineffective as well. However, our data base is by far too small to unambiguously identify such processes; measurements of the fluorescence light would be a necessity for their assignment.

The suppression of the H peak by surface layers can easily be understood, because all the molecules investigated here can sink electronic excitation within the energy

range above 9.7 eV either by getting ionized or excited, see above. We emphasize that for N_2 the rate depletion for the $a\ ^1\Pi_g \leftarrow X\ ^1\Sigma_g^+$ transition due to the dipole selection rules is widely canceled in the near-field regime important for the Förster-Dexter mechanism.[32]

The causes for the enhancement of the L maximum however are dubious. Reimann, Brown, and Johnson[10] observed luminescence from Ar/O_2 and Ar/N_2 layers which were related to the decay of the electronically excited state of ArN* and ArO*, respectively. This is an indication of the formation of intermediates *after* fragmentation of the added molecules (we emphasize that dissociation of the nitrogen molecule via quenching of Ar excitons seems very unlikely in agreement with Ref. 10; however, N_2 can well be dissociated by our fast electrons of 200 eV). In Ref. 10, the luminescence light was observed to increase with the ion exposure of the sample, i.e., ArN* and ArO* were formed in secondary steps. The formation and decay of such mixed dimers of Ar and fragments of molecules cannot be the reason for the enhanced desorption yield obtained here for NO and O_2 *from the start* of the irradiation, whereas extended bombardment causes its leveling off. Possibly the decay of excited compounds of Ar and the molecules, or larger clusters of these might be important. The maximum at 355 meV which is seen for 0.5 ML of NO on the surface, but not for 5% of NO in the bulk, and not for condensed NO either,[43] could be indicative of direct desorption by the decay of such Ar-NO entities.

We have shown that even for high electron doses the spectra characteristic for samples of clean Ar were never completely restored. This indicates that the atoms arising from the dissociation of the molecular additives influence energy diffusion and desorption as well; these findings are in good agreement with the luminescence data from Ref. 10.

In summary, we have investigated the influence of the metallic substrate, of crystallographic defects as well as of impurities on the desorption yield and the distributions of kinetic energy of desorbing Ar atoms for argon films. We found that the desorption rate fractions due to monolayer-derived DIET, molecular and cavity mechanism, respectively, strongly depend on film thickness. For the molecular mechanism, the branching into direct desorption and sputtering is a function of impurity and lattice defect density, which both suppressed the part of $N(E_k)$ related to the direct process. The influence of different molecules on the yield and $N(E_k)$ can be understood at least qualitatively. We conclude that the investigation of these "bulk" samples requires vacuum conditions that are as good as, or even better than, those commonly available in surface science experiments.

ACKNOWLEDGMENTS

We thank Y. Baba and D. Menzel for valuable discussions, and the latter also for critical advice, as well as for the possibility to perform these experiments in his laboratory. Experimental support by W. Friess, H. Schlichting, and W. Wurth is gratefully acknowledged. We thank E. Kellner for the preparation of the activated carbon layer of our time-of-flight apparatus. This study was funded by the Deutsche Forschungsgemeinschaft through Sonderforschungsbereich 338, and the synchrotron measurements by the German Ministry of Research and Technology, BMFT, through Project No. 05 466 CAB.

[1]P. R. Antoniewicz, Phys. Rev. B **21**, 3811 (1980).

[2]Q.-J. Zhang and R. Gomer, Surf. Sci. **109**, 567 (1981); Q.-J. Zhang, R. Gomer, and D. R. Bowman, *ibid* **129**, 535 (1983); E. R. Moog, J. Unguris, and M. B. Webb, *ibid.* **134**, 849 (1983); P. Feulner, D. Menzel, H. J. Kreuzer, and Z. W. Gortel, Phys. Rev. Lett. **53**, 671 (1984); Z. W. Gortel, H. J. Kreuzer, P. Feulner, and D. Menzel, Phys. Rev. B **35**, 8951 (1987); Z. W. Gortel, R. Teshima, and H. J. Kreuzer, *ibid.* **37**, 3183 (1988).

[3]Z. W. Gortel, Surf. Sci. **231**, 193 (1990); W. Hübner and K.-H. Bennemann, Z. Phys. B **78**, 131 (1990); R. E. Walkup, P. Avouris, N. D. Lang, and R. Kawai, Phys. Rev. Lett. **63**, 1972 (1989).

[4]Z. W. Gortel and A. Wierzbicki, Surf. Sci. **239**, L565 (1990).

[5]E. Steinacker and P. Feulner, Phys. Rev. B **40**, 11 348 (1989).

[6]R. E. Johnson and M. Inokuti, Nucl. Instrum. Methods **206**, 289 (1983); C. T. Reimann, R. E. Johnson, and W. L. Brown, Phys. Rev. Lett. **53**, 600 (1984).

[7]F. Coletti, J. M. Debever, and G. Zimmerer, J. Phys. Lett. **45**, L467 (1984); T. Kloiber, W. Laasch, G. Zimmerer, F. Coletti, and J. M. Debever, Europhys. Lett. **7**, 77 (1988).

[8]N. Schwentner, E.-E. Koch, and J. Jortner, *Electronic Excitations in Rare Gas Solids,* Springer Tracts in Modern Physics Vol. 107 (Springer, Berlin, 1985); G. Zimmerer, in *Excited State Spectroscopy in Solids,* edited by U. M. Grassano and N. Terzi (Società Italiana di Fisica, Bologna, 1987), p. 36.

[9]F. V. Kusmartsev and E. I. Rashba, Czech. J. Phys. B **32**, 54 (1982).

[10]C. T. Reimann, W. L. Brown, and R. E. Johnson, Phys. Rev. B **37**, 1455 (1988).

[11]T. Kloiber, Ph.D. thesis, Universität Hamburg, 1989.

[12]S. Cui, R. E. Johnson, and P. T. Cummings, Phys. Rev. B **39**, 9580 (1989).

[13]S. T. Cui, R. E. Johnson, C. T. Reimann, and J. W. Boring, Phys. Rev. B **39**, 12 345 (1989).

[14]W. T. Buller and R. E. Johnson, Phys. Rev. B **43**, 6118 (1991).

[15]H. Schlichting, Ph.D. thesis, Technische Universität München, 1991; H. Schlichting and D. Menzel (unpublished).

[16]B. J. Garrison and R. E. Johnson, Surf. Sci. **148**, 388 (1984).

[17]S. Cui, R. E. Johnson, and P. Cummings, Surf. Sci. **207**, 186 (1988).

[18]S. T. Cui, P. T. Cummings, and R. E. Johnson, Surf. Sci. **222**, 491 (1989).

[19]D. J. O'Shaughnessy, J. W. Boring, S. Cui, and R. E. Johnson, Phys. Rev. Lett. **61**, 1635 (1988).

[20]E. Steinacker, Diploma thesis, Technische Universität München, 1988; E. Steinacker, P. Feulner, and D. Menzel (unpublished).

[21]R. Pedrys, D. J. Oostra, and A. E. de Vries, in *Desorption Induced by Electronic Transitions, DIET II,* edited by W. Brenig and D. Menzel (Springer, Berlin, 1985), p. 190; R. Pedrys, D. J. Oostra, A. Haring, A. E. de Vries, and J. Schou, Nucl. Instrum. Methods B **33**, 840 (1988).

[22]J. W. Boring, R. E. Johnson, and D. J. O'Shaughnessy, Phys. Rev. B **39**, 2689 (1989).

[23]I. Arakawa, M. Takahashi, and K. Takeuchi, J. Vac. Sci. Technol. A **7**, 2090 (1989).

[24]C. T. Reimann, W. L. Brown, M. J. Nowakowski, S. T. Cui, and R. E. Johnson, in *Desorption Induced by Electronic Trasnsitions, DIET IV,* edited by G. Betz and P. Varga (Springer, Berlin, 1990), p. 226.

[25]J. F. O'Brian and K. J. Teegarden, Phys. Rev. Lett. **17**, 919 (1966); Z. Ophir, B. Raz, J. Jortner, V. Saile, N. Schwentner, E.-E. Koch, M. Skibowski, and W. Steinmann, J. Chem. Phys. **62**, 650 (1975); Z. Ophir, N. Schwentner, B. Raz, M. Skibowski, and J. Jortner, J. Chem. Phys. **63**, 1072 (1975).

[26]M. W. Thompson, Philos. Mag. **18**, 377 (1968).

[27]D. Menzel and R. Gomer, J. Chem. Phys. **41**, 3311 (1964).

[28]L. J. Kieffer, At. Data **1**, 19 (1969); L. J. Kieffer and G. H. Dunn, Rev. Mod. Phys. **38**, 1 (1966).

[29]J. Berkowitz, *Photoabsorption, Photoionization, and Photoelectron Spectroscopy* (Academic, New York, 1979), p. 155.

[30]R. Kink, A. Lohmus, and M. Selg, Phys. Status Solidi B **107**, 479 (1981).

[31]T. Förster, Ann. Phys. **2**, 55 (1948).

[32]D. L. Dexter, J. Chem. Phys. **21**, 836 (1953).

[33]F. Bozso, J. T. Yates, Jr., J. Arias, H. Metiu, and R. M. Martin, J. Chem. Phys. **78**, 4256 (1983); G. Schönhense, A. Eyers, and U. Heinzmann, Phys. Rev. Lett. **56**, 512 (1986).

[34]R. R. Chance, A. Prock, and R. Silbey, J. Chem. Phys. **62**, 2245 (1975).

[35]P. Feulner, T. Müller, A. Puschmann, and D. Menzel, Phys. Rev. Lett. **59**, 791 (1987).

[36]S. Bernstorff, Ph.D. thesis, Universität Hamburg, 1984.

[37]H. U. Böhmer and S. D. Peyerimhoff, Z. Phys. D **11**, 239 (1989); P. J. Kuntz and J. Valldorf, *ibid.* **8**, 195 (1988).

[38]H. U. Böhmer and S. D. Peyerimhoff, Z. Phys. D **3**, 195 (1986).

[39]P. Feulner, W. Riedl, and D. Menzel, Phys. Rev. Lett. **50**, 986 (1983).

[40]O. Ellegaard, P. Pedrys, J. Schou, H. Sorensen, and P. Borgesen, Appl. Phys. A **46**, 305 (1988).

[41]R. Scheuerer, P. Feulner, G. Rocker, L. Zhu, and D. Menzel, in *DIET IV,* edited by G. Betz and P. Varga (Springer, Berlin, 1990), p. 235.

[42]G. Herzberg, *Molecular Spectra and Molecular Structure* (Van Nostrand, Toronto, 1950), p. 501, Table 39; A. A. Radzig and B. M. Smirnov, *Reference Data on Atoms, Molecules, and Ions,* Springer Series in Chem. Phys. Vol. 31 (Springer, Berlin, 1985).

[43]E. Hudel, E. Steinacker, and P. Feulner (unpublished).